Probing quark gluon plasma in pA collisions

D M Adamiak[1,2]**,W A Horowitz**[1]

[1]Department of Physics, University of Cape Town, Private Bag X3, Rondebosch 7701, South Africa

E-mail: [2] daniel.m.adamiak@gmail.com

Abstract. We present novel predictions for the suppression of high momentum particles in high multiplicity proton-nucleus (pA) collisions at LHC. Shocking recent data from LHC demonstrates that high multiplicity pA collisions show signatures of the formation of a quark-gluon plasma (QGP), thought previously to only result from nucleus-nucleus collisions. Our work provides a new test of this QGP creation hypothesis.

We generate our predictions by first computing the initial spectrum of high momentum quarks and gluons using leading order (LO) perturbative quantum chromodynamics (pQCD). These LO pQCD predictions use both the usual parton distribution functions (PDFs) and nuclear PDFs, which encapsulate the modifications of the usual PDFs by the presence of multiple nucleons in a nucleus. We find that our results consistently describe the $p\bar{p}$ data at Fermilab, across multiple orders of magnitude in centre of mass energy $\sqrt{s}$, and over many orders of magnitude in transverse momentum. Next we implement state-of-the-art LO pQCD energy loss including radiative and collisional modes through a dynamical QGP medium. Finally, the particles are fragmented into hadrons and compared to the spectrum of high momentum particles in minimum bias pp collisions for future comparison with experimental data.

1. Introduction

Experiments from RHIC[1] and Cern[2] reveal a new state of matter that allow us to probe quantum chromo-dynamics (QCD). This state of matter is the quark-gluon-plasma (QGP). It occurred micro-seconds after the big-bang[3] and arises due to the emergent, many-body physics of QCD[4]. Successfully predicting and understanding QGP will give us an insight into these precesses.

The primary mechanism by which we will investigate QGP is that of parton pair production on near the edge of the QGP medium[5]. When partons are pair-produced, by conservation of momentum, they scatter back-to-back. One parton escapes escapes the QGP quickly and forms a jet largely unmitigated by the presence of a medium. The second parton has to travel through medium, where it undergoes radiative[6] and collisional[7] energy loss via interactions with the medium, eventually forming a jet with much lower energy than the first. These two jets may be compared, where the energy loss between the two may be used to deduce properties of the medium.

There are two prerequisites to performing energy-loss calculations. The first is that any and all non-energy-loss effects need to be under good theoretical control in order to not conflate between disparate effects. In particular, since there is strong evidence of QGP in nucleus nucleus collisions[8], the nuclear effects of interacting partons that arise from nuclei need to be taken into account. To the end of setting up this good theoretical control, careful analysis of proton anti-proton and proton nucleus collisions are presented.

The second prerequisite is that energy-loss calculations can only be performed for partons with known momenta. Therefore it is critical to obtain the spectra for the outgoing partons in these collisions. These spectra are also known as the partonic contributions to the total cross-section.

In this work we satisfy these two conditions, laying the groundwork for exploration into energy-loss, not only in nucleus nucleus collisions, but proton nucleus and proton proton collisions as well.

2. Leading Order pQCD Calculations

Using formulae derived from perturbative QCD (pQCD), we intend to calculate the inclusive spectra of charged hadron production from proton anti-proton and proton nucleus collisions. We also intend to lay the groundwork for energy-loss calculations that can be used to determine the presence of QGP in collider experiments.

This is done by calculating the differential cross-section of charged hadron production from these collisions, which has the following structure

$$\text{cross-section} = \text{PDF} \times \text{partonic cross-section} \times \text{energy-loss} \times \text{fragmentation}$$

where the terms on the right-hand side each describe a phase in the collision. The PDF (parton distribution function) describes partons incoming from their respective hadrons. The partonic cross-section describes the probability of them interacting in a particular way, e.g. the likely-hood of two gluons scattering into a quark anti-quark pair. After the parton scattering, the outgoing partons may then lose energy in the presence of a medium and it is this aspect of collisions by which we aim to probe the QGP. Finally, the outgoing partons fragment into hadrons.

It is vital to get the PDF and partonic cross-section correct in isolation, because they feed directly into the energy-loss and fragmentation. In other words, it would be impossible to discern effects due to energy-loss in isolation until we have a comprehensive understanding of all the non-energy-loss effects present in these heavy-ion collisions. To that end, we need to study collisions where we do not expect energy-loss or the presence of a medium. Proton anti-proton collisions serve this purpose. We also need to study nuclear effects, the difference in behaviour of partons that come from nuclei as opposed to single protons. The study of proton nucleus collisions serve this.

More details of each constituent to the cross-section are given in the next section.

2.1. $p\bar{p}$ collisions

Using Mathematica, we calculate the inclusive differential cross-section for production of a charged hadron h at a rapidity y from an proton anti-proton ($p\bar{p}$) collision. The expression for this cross-section, derived using pQCD, is given in [9]

$$\begin{aligned}\frac{d\sigma^{AB\to h+X}}{dq_T^2 dy} &= K(\sqrt{s})J(m_T,y)\int\frac{dz}{z^2}\int dy_2 \sum_{<ij><kl>}\frac{1}{1+\delta_{kl}}\frac{1}{1+\delta_{ij}}\times\\ &\times\Bigg\{x_1 f_{i/A}(x_1,Q^2)x_2 f_{j/B}(x_2,Q^2)\left[\frac{d\hat{\sigma}}{d\hat{t}}^{ij\to kl}(\hat{t},\hat{u})\underset{k\to h}{D}(z,\mu_F^2)+\frac{d\hat{\sigma}}{d\hat{t}}^{ij\to kl}(\hat{u},\hat{t})\underset{l\to h}{D}(z,\mu_F^2)\right]\\ &+\ x_1 f_{j/A}(x_1,Q^2)x_2 f_{i/B}(x_2,Q^2)\left[\frac{d\hat{\sigma}}{d\hat{t}}^{ij\to kl}(\hat{u},\hat{t})\underset{k\to h}{D}(z,\mu_F^2)+\frac{d\hat{\sigma}}{d\hat{t}}^{ij\to kl}(\hat{t},\hat{u})\underset{l\to h}{D}(z,\mu_F^2)\right]\Bigg\}\end{aligned} \tag{1}$$

where y_1 and y_2 are the rapidities of the final-state partons, k and l. The momentum fractions of the incoming partons are given by $x_1 = \frac{p_T}{\sqrt{s}}(e^{y_f} + e^{y_2})$ and $x_2 = \frac{p_T}{\sqrt{s}}(e^{-y_f} + e^{-y_2})$. z is a parameter equal to the ratio of the energy of the quark, f, to hadron h. $\sqrt{s}$ is the root center of mass energy, the energy in the rest frame of the interaction. Present are the differential cross-sections of parton interactions, $\frac{d\sigma}{d\hat{t}}$ and the Mandelstam variables, $\hat{t}, \hat{u}$. Also present are the parton distribution functions[10][11], f and fragmentation functions[12][13], D. J is the Jacobian of the change between pseudo-rapidity and rapidity, given by

$$J(m_T, y) = \left(1 - \frac{m^2}{m_T^2 \cosh^2 y}\right)^{-1/2} \tag{2}$$

where m is the mass of the outgoing hadron and m_T is the transverse mass of the outgoing hadron. The sum over i, j, k, l is a sum over every possible interaction, where i, j, k, l stand for labels of the different partons(quarks, anti-quarks and gluons). The constant, K, is the ratio of the experimental cross-section to the leading order cross-section. It was found by Eskola and Honkanen[9] that K was a function only of $\sqrt{s}$ and encapsulates the next-to-leading order contributions.

Intuitively, what is being described by this integral, is that the probability of h being formed at momentum q_T, is equal to the sum over every possible interaction that could form h with momentum q_T.

2.2. pA collisions

Using Mathematica, we calculate the differential cross-section for the production of charged hadrons for proton-nucleus (pA) collisions. We use the same calculation as for $p\bar{p}$ collisions, except one of the parton distribution functions of eq[1] are replaced with the nuclear parton distribution function[14] to indicate that the associated parton forms part of a larger nucleus, rather than a mere proton. These nuclear parton distribution functions encapsulate the nuclear effects that arise from involving nuclei in the collision.

2.3. Modification to extract partonic contributions

We now modify our calculation so that we can calculate the individual contribution to the total cross-section from each parton to serve as an input into future energy-loss calculations. The modification is quite simple. Examining eq[1], we eliminate the fragmentation functions, since these are used to tell us about the formation of hadrons. This leaves us with a calculation concerning the production of partons.

The second modification is that, rather than summing over all the partons, we record the contribution due to each parton separately. Our calculation then looks like

$$\begin{aligned} \frac{d\sigma^{AB\to k+X}}{dq_T^2 dy_f} &= \int dy_2 \sum_{<ij><kl>} \frac{1}{1+\delta_{kl}} \frac{1}{1+\delta_{ij}} \times \\ &\times x_1 f_{i/A}(x_1, Q^2) x_2 f_{j/B}(x_2, Q^2) \left[\frac{d\hat{\sigma}}{d\hat{t}}^{ij\to kl}(\hat{t}, \hat{u})\right] \end{aligned} \tag{3}$$

where, once again, i, j, k, l represent each of the participating partons where we now save the result for the k outgoing partons individually.

3. Results

3.1. $p\bar{p}$ cross-section

In order verify that eq[1] is valid, we compute the cross-section at $\sqrt{s} = 630$ GeV and compare to data.

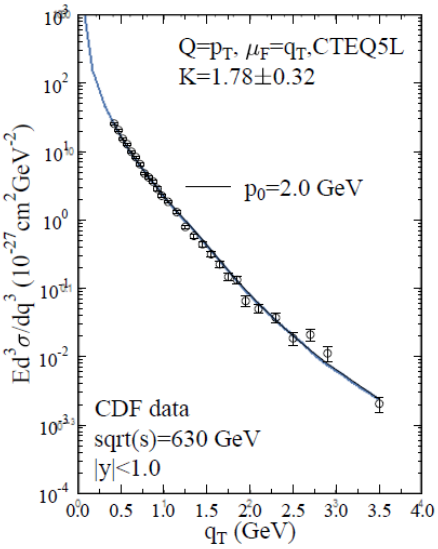

Figure 1. Differential cross-section of charged hadron production of a $p\bar{p}$ collision at $\sqrt{s} = 630$ GeV. The blue line is our calculation, the black line (over-lapping with the blue line) is the prediction from fig[5] of [9], where the data are taken.

Our calculation shows strong agreement with data and agrees with the prediction from [9] within numerical precision.

3.2. pA cross-section

In order to verify our understanding of the nuclear effects in scattering cross-section we calculate the differential cross-section of pA collision at $\sqrt{s} = 5.02$ TeV and compare with data from ALICE[15]

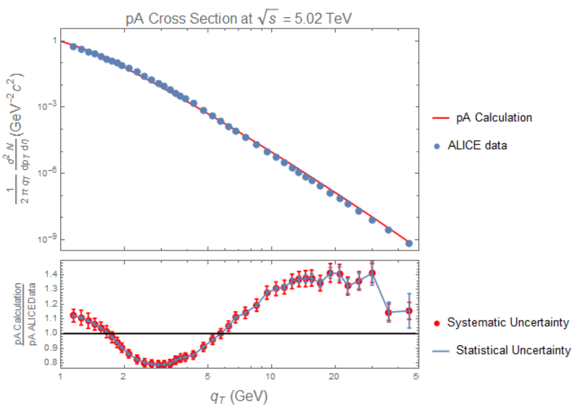

Figure 2. (Top) Plotted is the minimum bias inclusive differential cross-section of charged hadron production. The red line is our calculation, the blue points are data from ALICE. (Bottom) A ratio of our calculation to the data with systematic and statistical uncertainties.

We find that our calculation agrees with the data to within 40 percent. This is a strong agreement for a QCD calculation.

3.3. Partonic contribution

To serve as a critical input into energy loss calculations we find it useful to extract the partonic contributions from the above calculated cross-sections as calculated in eq[3]. As an example, we calculate the partonic contribution of a $p\bar{p}$ collision at $\sqrt{s} = 5.02$ TeV.

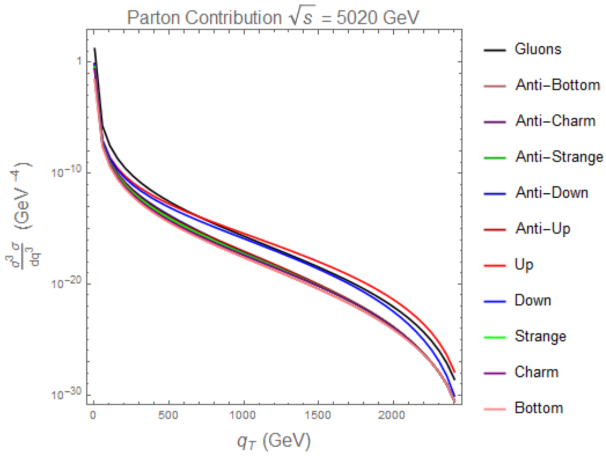

Figure 3. Spectra of each parton and their contribution to the total differential cross-section

4. Discussion

The goal of this work was to establish good theoretical control over the non-energy loss processes that occur in collisions. Figure 1 shows that we can accurately predict the result of $p\bar{p}$ collisions. This demonstrates an understanding of the partonic processes, the interaction between partons in these collisions, as well as the fragmentation process into hadrons. Figure2 shows that we are able to predict the result of pA collisions. Since the only effects we included into our calculation that differ from the $p\bar{p}$ calculation are the nuclear effects and the fact that we have such strong agreement with data, indicate that we have good theoretical control over the nuclear effects.

We have also demonstrated the ability to extract the partonic contribution to the cross-section. We have confidence in this result because, in the absence of energy-loss (such as in $p\bar{p}$ collisions), the partonic contribution serves as a direct input into the fragmentation process, which gives the total differential cross-section of fig 1.

5. Outlook

The techniques of pQCD have shown to be apt when it comes to the prediction of differential cross-sections of charged hadron production. We have confidence that non-energy-loss effects are under good control. The stage is set to perform energy-loss calculation to probe the presence of a QGP. The most obvious avenue to do this is for AA collisions, but recent research suggests that high-multiplicity cuts of pp and pA collisions show characteristics of possessing a medium [16]. This presents the perfect opportunity to apply energy-loss calculations to pp and pA collisions, where the presence of QGP has not been confirmed, but could serve as a new probe into this medium.

6. Acknowledgments

I would like to thank the Harry Crossley foundation for supporting me financially throughout this endeavor.

References

[1] Miklos Gyulassy and Larry McLerran. Quark-gluon plasma. new discoveries at rhic: Case for the strongly interacting quark-gluon plasma. contributions from the rbrc workshop held may 14-15, 2004 new forms of qcd matter discovered at rhic. *Nuclear Physics A*, 750(1):30 – 63, 2005.

[2] Thomas Ullrich, Bolek Wysouch, John W. Harris, and Urs Achim Wiedemann. The quark matter 2012 introductory overview of quark matter 2012. *Nuclear Physics A*, 904:3c – 10c, 2013.

[3] K. Kajantie and Hannu Kurki-Suonio. Bubble growth and droplet decay in the quark-hadron phase transition in the early universe. *Phys. Rev. D*, 34:1719–1738, Sep 1986.

[4] The Frontiers of Nuclear Science, A Long Range Plan. 2008.

[5] Miklos Gyulassy, Peter Levai, and Ivan Vitev. Jet quenching in thin plasmas. *Nucl. Phys.*, A661:637–640, 1999.

[6] Magdalena Djordjevic and Marko Djordjevic. Generalization of radiative jet energy loss to non-zero magnetic mass. *Phys. Lett.*, B709:229–233, 2012.

[7] Magdalena Djordjevic. Collisional energy loss in a finite size QCD matter. *Phys. Rev.*, C74:064907, 2006.

[8] Julia Velkovska. What have hard probes taught us about the quarkgluon plasma as measured in cms? *Nuclear Physics A*, 932:17 – 24, 2014. Hard Probes 20136th International Conference on Hard and Electromagnetic Probes of High-Energy Nuclear Collisions.

[9] K. J. Eskola and H. Honkanen. A Perturbative QCD analysis of charged particle distributions in hadronic and nuclear collisions. *Nucl. Phys.*, A713:167–187, 2003.

[10] M Dittmar, S Forte, A Glazov, S Moch, S Alekhin, Guido Altarelli, J Andersen, R D Ball, J Blmlein, Helmut B Bttcher, T Carli, Marcello Ciafaloni, D Colferai, A Cooper-Sarkar, Gennaro Corcella, L Del Debbio, G Dissertori, J Feltesse, A Guffanti, C Gwenlan, J Huston, G Ingelman, M Klein, J I Latorre, T Lastoviicka, G Lastoviicka-Medin, L Magnea, A Piccione, J Pumplin, V Ravindran, B Reisert, J Rojo, Agustin Sabio Vera, Gavin P Salam, F Siegert, A M Stasto, H Stenzel, C Targett-Adams, R S Thorne, A Tricoli, J A M Vermaseren, and A Vogt. Introduction to parton distribution functions. 2005.

[11] H. L. Lai, J. Huston, S. Kuhlmann, J. Morfin, Fredrick I. Olness, J. F. Owens, J. Pumplin, and W. K. Tung. Global QCD analysis of parton structure of the nucleon: CTEQ5 parton distributions. *Eur. Phys. J.*, C12:375–392, 2000.

[12] D de Florian and D Milstead. 17. fragmentation functions in e e-, ep and pp collisions.

[13] Bernd A. Kniehl, G. Kramer, and B. Potter. Fragmentation functions for pions, kaons, and protons at next-to-leading order. *Nucl. Phys.*, B582:514–536, 2000.

[14] K. J. Eskola, H. Paukkunen, and C. A. Salgado. EPS09: A New Generation of NLO and LO Nuclear Parton Distribution Functions. *JHEP*, 04:065, 2009.

[15] K. Aamodt et al. Suppression of Charged Particle Production at Large Transverse Momentum in Central Pb-Pb Collisions at $\sqrt{s_{NN}} = 2.76$ TeV. *Phys. Lett.*, B696:30–39, 2011.

[16] Georges Aad et al. Centrality and rapidity dependence of inclusive jet production in $\sqrt{s_{\mathrm{NN}}} = 5.02$ TeV proton-lead collisions with the ATLAS detector. *Phys. Lett.*, B748:392–413, 2015.